HO-1–Mediated Autophagic Restoration Protects Lens Epithelial Cells Against Oxidative Stress and Cellular Senescence

Lijun Wang, Wei Lou, Yao Zhang, Ziang Chen, Yang Huang, and Haiying Jin

Department of Ophthalmology, Shanghai East Hospital, School of Medicine, Tongji University, Shanghai, China

Correspondence: Haiying Jin, Department of Ophthalmology, Shanghai East Hospital, School of Medicine, Tongji University, Shanghai 200092, China; eagle_jin@163.com.
Yang Huang, Department of Ophthalmology, Shanghai East Hospital, School of Medicine, Tongji University, Shanghai 200092, China; huangyangaibb@163.com.

Received: April 9, 2023
Accepted: November 13, 2023
Published: December 5, 2023

Citation: Wang L, Lou W, Zhang Y, Chen Z, Huang Y, Jin H. HO-1–Mediated autophagic restoration protects lens epithelial cells against oxidative stress and cellular senescence. *Invest Ophthalmol Vis Sci.* 2023;64(15):6. https://doi.org/10.1167/iovs.64.15.6

Purpose. Oxidative stress and cellular senescence are risk factors for age-related cataract. Heme oxygenase 1 (HO-1) is a critical antioxidant enzyme and related to autophagy. Here, we investigate the crosstalk among HO-1, oxidative stress, and cellular senescence in mouse lens epithelial cells (LECs).

Methods. The gene expression of HO-1, p21, LC3, and p62 was measured in human samples. The protective properties of HO-1 were examined in hydrogen peroxide (H_2O_2)–damaged LECs. Autophagic flux was examined by Western blot and mRFP-GFP-LC3 assay. Western blotting and lysotracker staining were used to analyze lysosomal function. Flow cytometry was used to detect intracellular reactive oxygen species and analyze cell cycle. Senescence-associated β-galactosidase assay was used to determine cellular senescence. The crosstalk between HO-1 and transcription factor EB (TFEB) was further observed in TFEB-knockdown cells. The TFEB binding site in the promoter region of *Hmox1* was predicted by the Jasper website and was confirmed by chromatin immunoprecipitation assay.

Results. HO-1 gene expression decreased in LECs of patients with age-related nuclear cataract, whereas mRNA expression levels of p21, LC3, and p62 increased. Upon H_2O_2-induced oxidative stress, LECs showed the characteristics of autophagic flux blockade, lysosomal dysfunction, and premature senescence. Interestingly, HO-1 significantly restored the impaired autophagic flux and lysosomal function and delayed cellular senescence. TFEB gene silencing greatly reduced the HO-1–mediated autophagic restoration, leading to a failure to prevent LECs from oxidative stress and premature senescence.

Conclusions. We demonstrated HO-1 effects on restoring autophagic flux and delaying cellular senescence under oxidative stress in LECs, which are dependent on TFEB.

Keywords: age-related cataract, autophagy, heme oxygenase 1, TFEB, senescence

Cataract is the leading cause of visual impairment around the world.[1,2] To date, the only effective treatment is surgery, which results in heavy socioeconomic burden and the unavoidable risk of surgical complications. Moreover, cataract surgeries are not accessible for many patients in developing countries.[3] The nearly complete lack of effective medication drives a continuing demand for research on cataract pathogenesis.

Age-related cataract (ARC) constitutes most cases of cataract, which is a typical senescence-related ocular disorder that often affects persons over the age of 50.[1,4,5] The single-layered lens epithelial cells (LECs), distributed behind the anterior lens capsule, are the antioxidant activity center of the lens and have a major function in maintaining lens transparency.[6] Cellular senescence can be triggered by oxidative stress, and it is depicted as an irreversible cell cycle withdrawal accompanied by metabolic dysregulation, macromolecular damage, and senescence-associated secretory phenotype.[7,8] Although the pathogenesis of ARC is still largely unclear, it is widely accepted that reactive oxygen species (ROS), specifically hydrogen peroxide (H_2O_2), is the primary cause of epithelial cell damage and protein degradation.[9–11] In addition, premature senescence of LECs can be induced by exposure to a nonlethal dose of H_2O_2.[12,13]

Authophagy is a lysosome-dependent bulk degradation procedure that is essential for intracellular protein and organellar homeostasis.[14] Autophagic activity decreases with age, and impaired autophagy may have association with accelerated aging.[14–16] Autophagic lens defects generate cataracts in animal models.[17,18] Transcription factor EB (TFEB) is known as a pivotal transcriptional regulator of lysosomal function and autophagy.[19] Recent studies showed that TFEB-dependent lysosomal dysfunction inhibited autophagy activity in LECs, which might contribute to the formation of diabetic cataract.[20,21] Nevertheless, little is known in ARCs, and further study is needed on the crosstalk between autophagy, oxidative stress, and senescence in LECs.

Heme oxygenase 1 (HO-1) is one of key metabolic enzymes with robust cytoprotective effects on various stressors.[22,23] Previously, we have demonstrated that HO-1 and

its by-products, including biliverdin and carbon monoxide (CO), could protect LECs from oxidative stress and apoptosis.[24–26] The HO-1 expression level showed an age-dependent decrease among mouse LECs, and overexpression of HO-1 attenuated H_2O_2-induced oxidative stress, which means HO-1 could exert a vital role in the formation of ARC.[27] Moreover, there is growing evidence suggesting that autophagy and HO-1 are coregulated.[28] However, the nature of this relationship has yet to be elucidated in a cataract model.

In this investigation, we examined mRNA expression levels of HO-1, the senescence-associated marker p21, and autophagy-associated markers LC3 and p62 in LECs of age-related nuclear cataract (ARNC), which is closely associated with oxidative damage. Cobalt protoporphyrin (CoPP) and zinc protoporphyrin (ZnPP) acted as a HO-1 inducer and inhibitor, separately.[29] Thus, CoPP and ZnPP were used to explore how HO-1 plays a role under H_2O_2-induced oxidative stress in mouse LECs, and its relationships with cellular autophagy and senescence were investigated.

Materials and Methods

Human Samples

ARNC patient anterior lens capsules (n = 18 eyes) and noncataract participants (n = 18 eyes) were collected from Shanghai East Hospital. The noncataract specimens were from the age- and gender-matched presbyopia patients who received clear lens extraction, acting as the ARNC group's negative controls. All participants received a detailed ophthalmic examination and were evaluated with the Lens Opacities Classification System version III (LOCS III) by two independent examiners (J.H.Y. and H.Y.). The enrollment criteria for patients with ARNC were (1) more than 50 years of age and (2) N score greater than 3 without obvious cortical and subcapsular opacities determined by slit-lamp biomicroscopy. Exclusion criteria applied to all participants were (1) congenital, metabolic, and traumatic cataracts; (2) high myopia, uveitis, retinal disorders, and other ocular diseases; (3) previous intraocular surgeries; and (4) systemic disorders like diabetes mellitus. The demographic data of these participants are displayed in the Table.

Human anterior lens capsule tissue samples were obtained by an ophthalmologist (J.H.Y.) through the anterior continuous curvilinear capsulorhexis (CCC) from the central polar region of the lens during cataract surgery. The size of the CCC was approximately 5.5 to 6.0 mm in diameter. Then, the tissue samples were immediately frozen in liquid nitrogen and stored at −80°C for quantitative PCR (qPCR). Shanghai East Hospital's Ethical Review Board approved this study, which followed the Declaration of Helsinki. Each participant provided a signed informed consent.

Table. Patient Demographics With or Without Senile Cataract

Characteristic	ARNC (n = 18)	Noncataract (n = 18)	P Value
Age (y)	62.67 ± 4.03	63.94 ± 3.84	0.337*
Gender (male/female)	10/8	7/11	0.317†

* Student's t-test.
† Chi-square test.

Reagents

H_2O_2 (1.08600), CoPP (C1900), and ZnPP (691550-M) were acquired from Sigma-Aldrich (St. Louis, MO, USA). Bafilomycin-A1 (Baf-A1; HY-100558) was acquired from MedChemExpress (Monmouth Junction, NJ, USA). The cellular ROS assay kit (S0033M) and the senescence-associated β-galactosidase (SA-β-Gal) staining kit (C0602) were bought from Beyotime (Shanghai, China). The propidium iodide flow cytometry kit (ab14083) and the nuclear extraction kit (ab113474) were acquired from Abcam (Shanghai, China). TRIzol reagent (15596026) and SYBR Green (A25741) were purchased from Thermo Fisher Scientific (Shanghai, China). Anti–HO-1 antibody (ab189491), anti-LC3B (ab192890), anti-p62 (ab109012), anti–LAMP-1 (ab208943), anti-TFEB (ab264421), anti-p21 (ab188224), anti-p53 (ab26), anti–cyclin D1 (ab16663), anti-GAPDH (ab8245), and anti–Histone H3 (ab1791) primary antibodies were supplied from Abcam. Lipofectamine 3000 (L3000001), mRFP-GFP-LC3 adenovirus (P36239), and LysoTracker Green DND-26 (L7526) were acquired from Thermo Fisher Scientific.

Cell Culture

Previously, we described the procedures for the primary mouse LEC culture.[30] Briefly, lens capsule epithelium specimens were obtained from normal C57BL/6 mice (2 months old, 20–25 g), which were supplied from Beijing Long'An Animal Center (China). These specimens were sliced into 1-mm × 1-mm pieces and cultivated through Dulbecco's modified Eagle's medium that contained 2% fetal bovine serum. After cells migrated out of capsules, they were digested and collected for further procedures.

Cell Transfection

LECs were seeded in six-well plates (5×10^5 cells/well) and transfected until 70% confluency. Thermo Fisher Scientific provided small interfering RNAs (siRNAs) and empty vector (pcDNA3.1). Sequences of the siRNA targeting TFEB (siTFEB) were sense: 5′-GGTCTTGGGCAA ATCCCTT-3′; antisense: 5′-AAGGGATTTGCCCAAGACC-3′. Sequences of the siRNA targeting HO-1 (siHO-1) were sense: 5′-CCGAGAATGCTGAGTTCAT-3′; antisense: 5′-ATGAACTCAGCATTCTCGG-3′. Sequences of the negative control siRNA (siNC) were sense: 5′-TTCTCCGAACGTGTCAC GT-3′; antisense: 5′-ACGTGACACGTTCGGAGAA-3′. Then, 7 µL siTFEB or siHO-1 mixed with 5 µL Lipofectamine 3000 was used for siTFEB or siHO-1 single transfection. Next, 7 µL siTFEB, 7 µL siHO-1, and 5 µL Lipofectamine 3000 were mixed together for siTFEB/siHO-1 cotransfection. The plasmid for overexpressing HO-1 (pcDNA3.1-HO-1) was synthesized by BoRui Co., Ltd (Beijing, China). Then, 14 µg recombinant plasmid and empty vector (pcDNA3.1-NC) were respectively mixed with 10 µL Lipofectamine 3000. LECs were transfected with different transfection complexes for 6 hours at 37°C with 5% CO_2. The medium was then replaced with normal medium. Following 24 hours posttransfection, transfection efficacy was assessed using qPCR.

Cytoplasmic and Nuclear Protein Extraction

The processes were performed following the instructions of the nuclear extraction kit. In brief, after washing LECs with

Investigative Ophthalmology & Visual Science

ice-cold phosphate-buffered saline (PBS) twice, we added 500 µL PBS to each well of a six-well plate and scraped cells into a centrifuge tube, which were then centrifuged at a speed of 1000 rpm for 5 minutes. The supernatant was discarded, while the cell pellet was resuspended in preextraction buffer on ice for 10 minutes. After vigorous vortex for 10 seconds and centrifugation at 12,000 rpm for 1 minute, the nuclear and cytosolic extracts were centrifuged at 12,000 rpm for 1 minute, and the supernatant was removed to obtain the cytoplasmic extract. The nuclear pellet was washed three times and then resuspended in extraction buffer on ice for 15 minutes with vortex every 3 minutes. After centrifugation at 14,000 rpm for 10 minutes, the supernatants were collected to obtain nuclear protein extract.

Flow Cytometry

The intracellular ROS levels along with cell cycle were detected using flow cytometry (BD FACSAria, San Jose, CA, USA), and FlowJO 7.6 was used in the data analysis. For intracellular ROS detection, treated LECs were stained with 10 µM 2′,7′-dichlorofluorescein diacetate probe at 37°C in the dark for 20 minutes. After cells were rinsed twice with PBS, we measured fluorescence intensity at 488 nm. To analyze cell cycle, a propidium iodide flow cytometry kit was used following the manufacturer's protocol. After that, 1×10^5 cells were collected, centrifuged, and resuspended in 200 µL propidium working solution containing RNase A in darkness at 37°C for 30 minutes. Similarly, we measured fluorescence intensity at 488 nm.

SA-β-Gal Assay

The assay was conducted using SA-β-Gal stain kit. Following the protocol, LECs were washed, fixed, and then incubated with staining solution overnight at 37°C. LECs stained positively for SA-β-Gal were observed and quantified with a regular light microscope.

mRFP-GFP-LC3 Assay

LECs were grown on 12-well plates (2.5×10^5 cells/well) and incubated for 12 hours before transfection. LECs were transfected with mRFP-GFP-LC3 adenovirus as per the manufacturer's guidelines. A day after transfection, LECs were incubated with different treatments. Autophagy was observed using fluorescence microscopy, and autophagy flux was assessed by calculating green fluorescent protein (GFP) and monomeric red fluorescent protein (mRFP) puncta numbers.

Western Blotting

The protein of treated or untreated primary mouse LECs was extracted in lysis buffer. Equal amounts of proteins were size fractionated by 10% SDS-PAGE. Proteins were then translocated to polyvinylidene difluoride filter membranes (Millipore, Bedford, MA, USA). After being blocked with blocking buffer (5% nonfat milk), the membranes were then incubated with HO-1 (1:1000), TFEB (1:1000), p21 (1:1000), p53 (1:1000), cyclin D1 (1:1000), LC3 (1:1000), p62 (1:1000), and LAMP-1 (1:1000) at 4°C overnight. After incubation of horseradish peroxidase–conjugated secondary antibody, ImageJ software (v1.40; National Institutes of Health, Bethesda, MD, USA) was used to analyze the protein bands. GAPDH and H3 were employed separately as loading controls.

qPCR

An ultrasonic homogenizer was used to homogenize lens capsule specimens. Total RNA was isolated from each sample with the TRIzol kit, followed by the evaluation of RNA concentration and purity. After reverse transcription, qPCR was performed using SYBR Green as a fluorescent dye. Using the $2^{-\Delta\Delta Ct}$ technique, relative gene expression ws assessed and normalized to GAPDH expression housekeeping gene. Primer sequences are provided in Supplementary Table S1.

Chromatin Immunoprecipitation Assay

The chromatin immunoprecipitation (ChIP) assay was carried out with a EZ-ChIP ChIP Kit (17-408; Millipore). In brief, cells were fixed with 1% methanol. The ultrasound was used to shear the cross-linked DNA into 200- to 1000-bp small fragments, followed by incubating with Protein G magnetic beads in a shaker for 1 hour at 4°C. Subsequent to centrifugation at 6500 rpm for 1 minute, the supernatant was incubated with TFEB antibodies (ab264421, 1:1000; Abcam), H2A.X antibodies (ab124781, 1:1000; Abcam), or anti-rabbit immunoglobulin G (IgG) antibodies (A7016, 1:100; Beyotime) at 4°C. The antibody–chromatin complexes were separately added with Protein G magnetic beads and then cultured for 1 hour at 4°C. After centrifugation, the supernatant was removed and 100 µL eluent was mixed with the antibody–DNA complexes gently and placed for 15 minutes at room temperature. Then, the DNA was decrosslinked and purified. The fragment region of the predicative binding sites on the *Hmox1* promoter was amplified by PCR with the DNA extracted from TFEB antibody-immunoprecipitated chromatin fragments. Primers targeting promoter sequences were as follows: 5′-CGA GTT ACC GCC CAG TCT AC-3′ (forward) and 5′-CGC CAG CAA AAG ACA AGC TC-3′ (backward).

Statistical Analysis

PASS version 15 (NCSS, LLC, Kaysville, UT, USA) was used to assess sample size of participants enrolled in the research. Statistical analysis was done with GraphPad Prism 8 (GraphPad Software, San Diego, CA, USA) and data were represented as mean ± SEM. ANOVA or chi-square test combined with post hoc least significant difference test was used to compare several groups. The cutoff for statistical significance was set at $P < 0.05$. Each experiment was repeated three times.

Results

Decreased Expression of HO-1 and Increased Expression of p21, LC3, and p62 in the Lens Capsules of Patients With ARNC

In comparison with noncataract patients, HO-1 gene expression decreased in the ARNC samples ($P = 0.034$, Fig. 1A). However, the levels of p21 (senescence-associated marker), LC3 (autophagosome marker), and p62 (autophagy substrate marker) all increased in the samples from patients with ARNC compared to controls ($P = 0.022$, $P = 0.012$, $P = 0.037$,

Investigative Ophthalmology & Visual Science

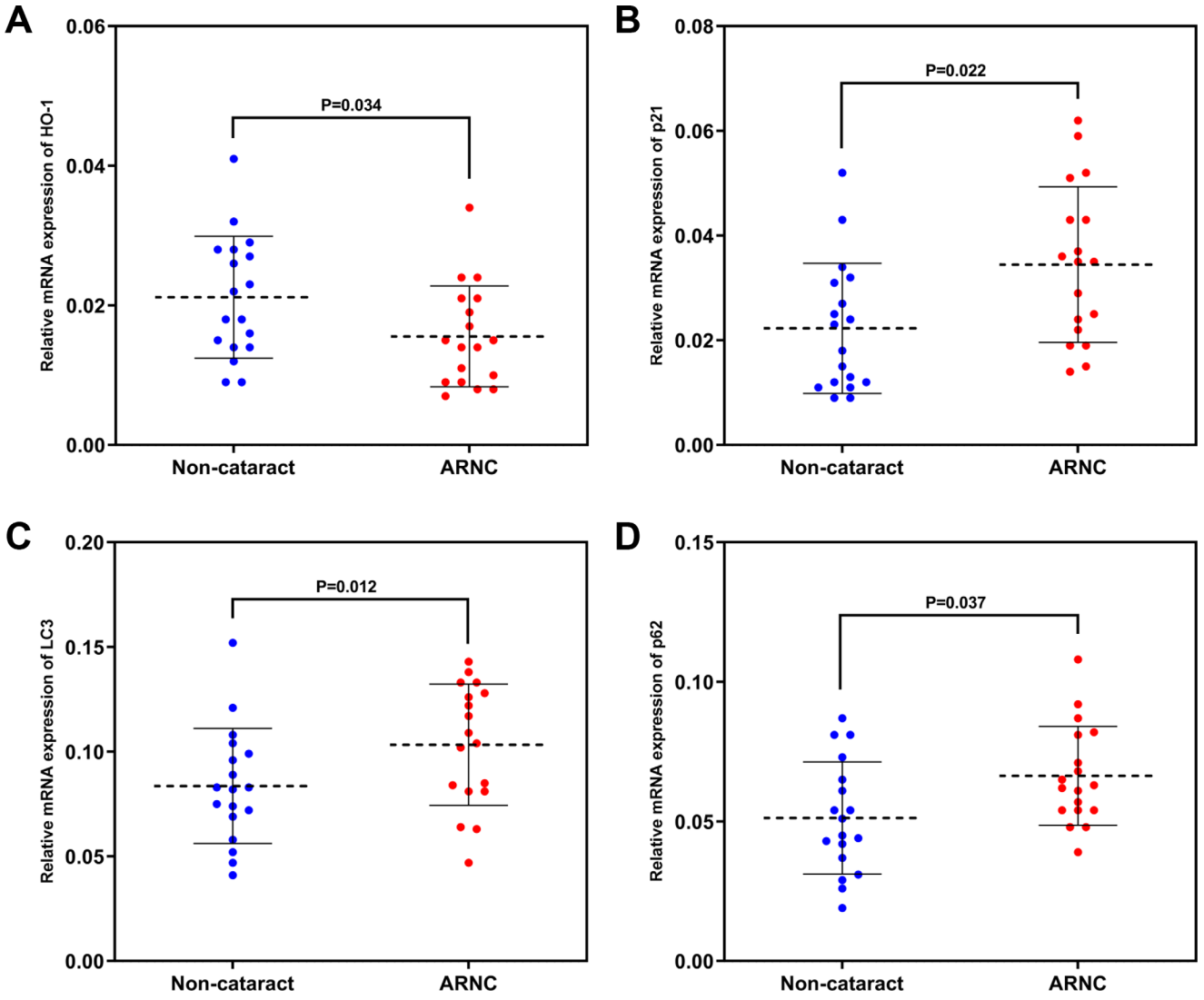

Figure 1. The relative mRNA levels of HO-1, p21, LC3, and p62 in the LECs of patients with ARNC and noncataract participants were detected by qPCR. $n = 18$ in each group.

Figs. 1B–D). Based on increases in both LC3 and p62, we speculated that autophagy is activated in LECs of patients with ARNC, but its completion is impeded due to decreased cargo degradation, resulting in impaired autophagic flux.

HO-1 Protects LECs From Premature Senescence Induced by Oxidative Stress

To determine the antioxidative property of HO-1, LECs were preconditioned with 10 µM CoPP or ZnPP for 6 hours before being exposed to 100 µM H_2O_2 for 7 days. We compared the intracellular ROS levels in each group. As shown in Figure 2A, H_2O_2 treatment increased the intracellular ROS levels to nearly fourfold compared to the control group ($P < 0.001$). In comparison with H_2O_2-treated group, pretreatment with CoPP decreased the ROS levels by almost half ($P < 0.05$), whereas the ZnPP preconditioning increased the ROS levels to about 1.5-fold ($P < 0.05$).

Then, HO-1 impacts on H_2O_2-induced premature senescence were investigated. Cell cycle analysis demonstrated that LECs could be retarded in the G0/G1 phase after 100 µM H_2O_2 treatment or 10 µM ZnPP treatment in comparison with the controls (both $P < 0.01$). In contrast to the H_2O_2-treated group, the cell percentage in the S phase increased, whereas the percentage in the G0/G1 phase decreased in the CoPP-pretreated group (both $P < 0.05$). However, ZnPP pretreatment aggravated the situation of cell cycle arrest in H_2O_2-exposed LECs (Fig. 2B). Furthermore, the levels of cyclin D1, which is known as a vital cell cycle factor regulating transition from the G1 to S phase,[31] decreased in H_2O_2-incubated LECs, which was restored by CoPP pretreatment and further downregulated by ZnPP pretreatment. Additionally, ZnPP treatment alone also decreased the cyclin D1 level in a moderate way. p21 and p53 expression levels were also analyzed, which are implicated in cell cycle arrest and activated in senescent cells.[32] ZnPP and H_2O_2 treatment alone led to elevated levels of p21 and p53 in contrast to the control group (all $P < 0.001$). Moreover, in H_2O_2-exposed LECs, CoPP pretreatment led to the upreg-

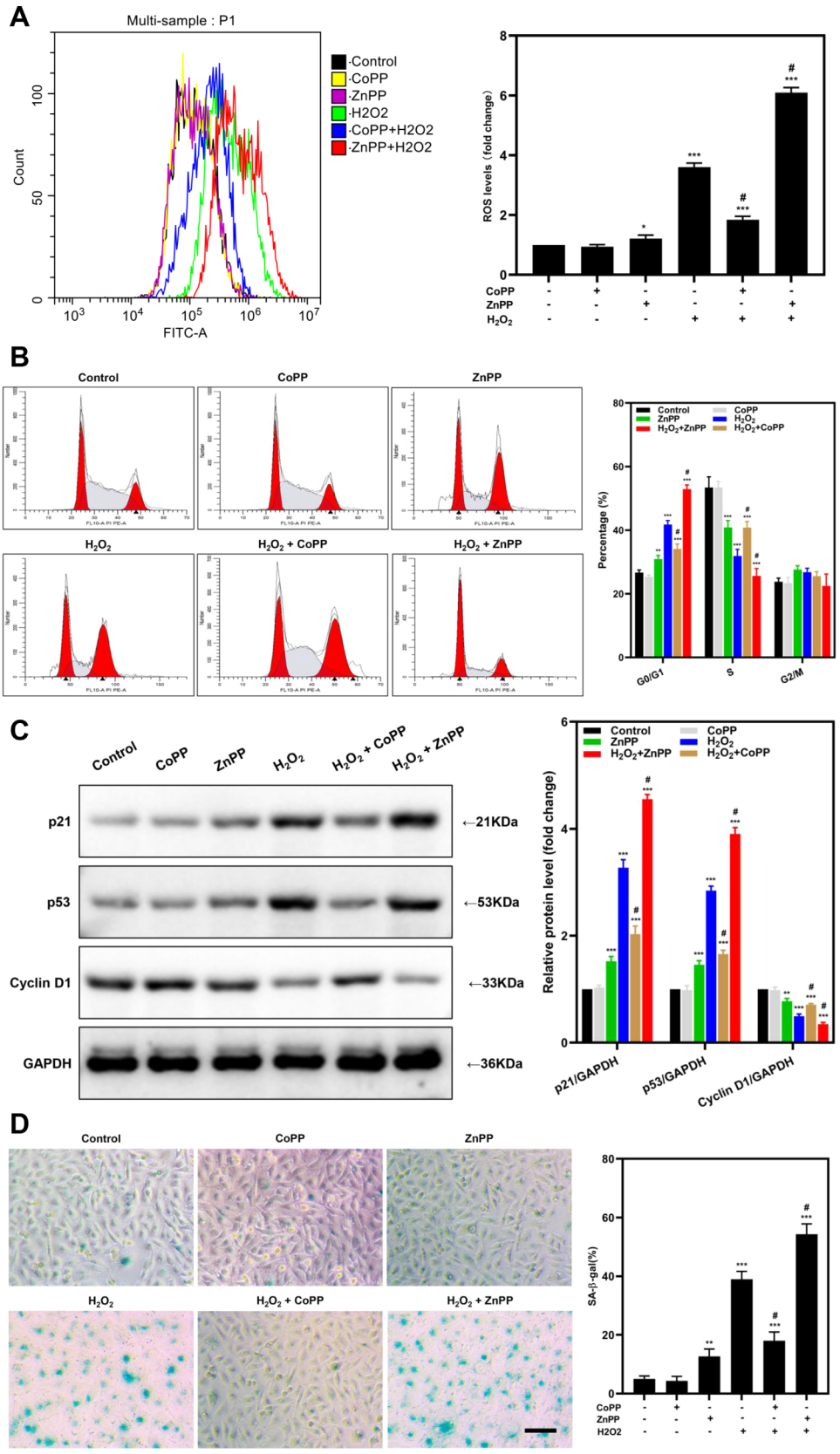

Figure 2. HO-1 prevents oxidative stress from senescence in LECs. The primary mouse LECs were treated with 10 µM CoPP or ZnPP for 6 hours or pretreated with 10 µM CoPP or ZnPP for 6 hours before being exposed to 100 µM H_2O_2 for 7 days. (**A**) 2′,7′-Dichlorofluorescein diacetate (DCFH-DA) staining was used to detect intracellular ROS levels in each group. (**B**) Cell cycle transition in LECs was determined by PI labeling. (**C**) WB was used to detect cell cycle regulator expression (p21, p53, and cyclin D1). GAPDH was used as loading controls. (**D**) SA-β-gal staining was used to analyze senescent cells percentage. $N = 3$, one-way ANOVA, $^{*}P < 0.05$, $^{**}P < 0.01$, $^{***}P < 0.001$, compared with the control group; $^{\#}P < 0.05$ compared with H_2O_2-treated group. *Bar*: 50 µm.

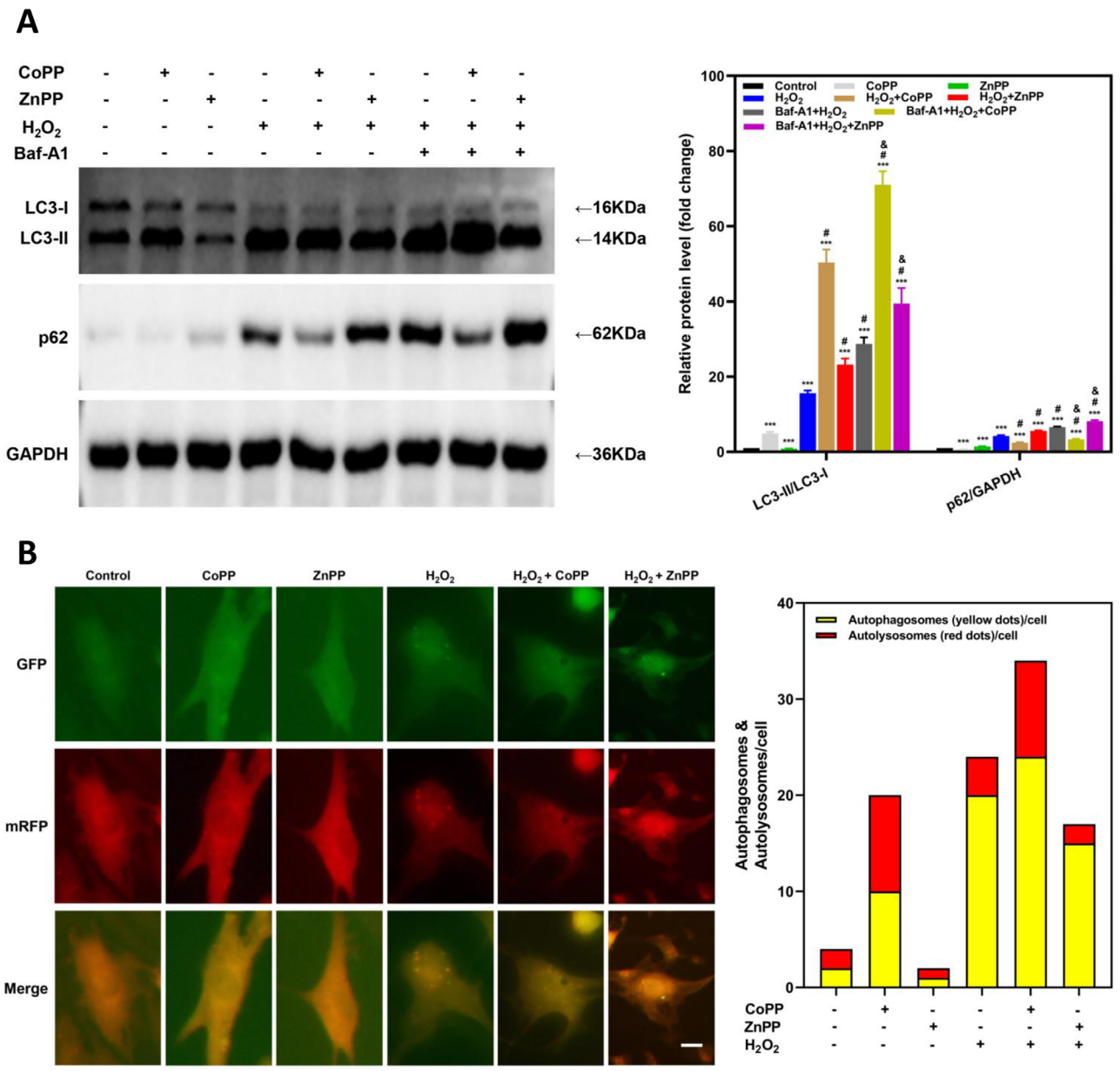

Figure 3. HO-1 enhances autophagy and promotes autophagic flux in LECs. (**A**) The primary mouse LECs were treated with 10 µM CoPP or ZnPP for 6 hours or pretreated with 10 µM CoPP or ZnPP for 6 hours before exposure to 100 µM H_2O_2 for 7 days with or without the addition of Baf-A1. WB was used to assess protein expression of LC3 and p62 following various treatments. GAPDH was used as a loading control. (**B**) mRFP-GFP-LC3 was transfected into the primary mouse LECs followed by different treatments, and fluorescent puncta were quantified per cell. Representative confocal microscopy images are shown. $n = 3$, one-way ANOVA, $^{***}P < 0.001$, compared with control group; $^{\#}P < 0.05$ compared with H_2O_2-treated group; $\&P < 0.05$ compared with H_2O_2-Baf-A1–treated group. *Bar*: 20 µm.

ulation of p21 and p53 while ZnPP pretreatment further decreased p21 and p53 levels (Fig. 2C). Obviously, SA-β-gal staining assay showed that ZnPP and H_2O_2 alone both promoted the expression of senescence marker SA-β-gal. In H_2O_2-treated groups, CoPP pretreatment decreased SA-β-gal–positive cells percentage, whereas ZnPP pretreatment promoted LEC senescence (Fig. 2D). These results showed that HO-1 effectively suppressed premature senescence induced by oxidative stress.

HO-1 Restores Autophagy Flux Impaired by H_2O_2

To investigate whether HO-1 is involved in autophagy in LECs, we treated LECs with 10 µM CoPP or ZnPP for 6 hours and detected the early-stage autophagy markers by Western blot (WB), including LC3 and p62. In contrast to the control group, CoPP treatment alone increased the LC3-II/LC3-I ratio and decreased the p62 expression level ($P < 0.001$), which implied that the induction of HO-1 promotes the formation and maturation of autophagosomes. However, inhibiting HO-1 function by ZnPP reversed the effects. Although exposure to 100 µM H_2O_2 for 24 hours facilitated a higher level of LC3-II/LC3-I, p62 was accumulated compared with the control group. LECs were preconditioned with 10 µM CoPP or ZnPP for 6 hours before exposure to 100 µM H_2O_2 for 7 days to further evaluate HO-1 effects on H_2O_2-induced autophagy. Intriguingly, CoPP pretreatment promoted LC3-II/LC3-I conversion and p62 degradation

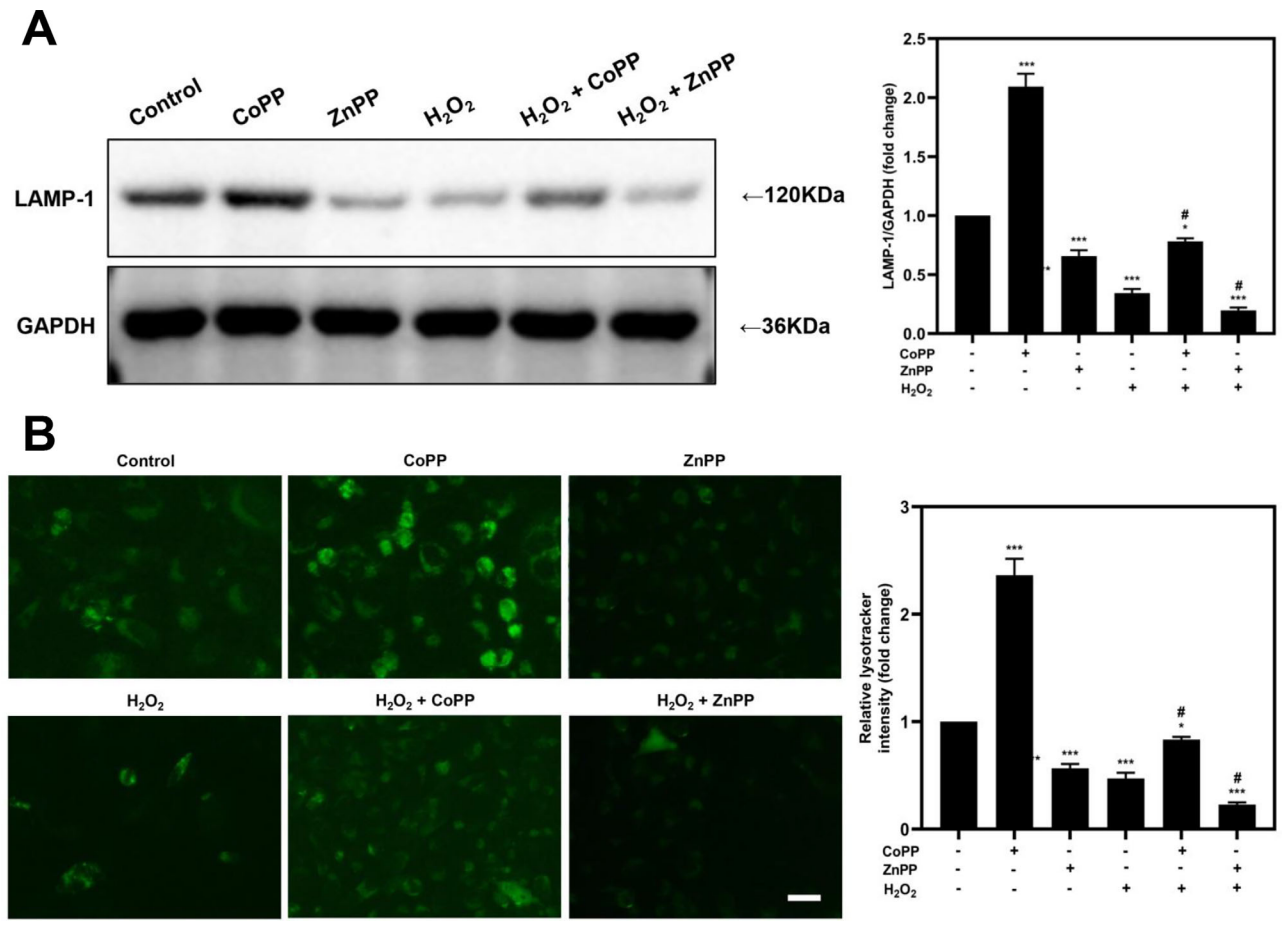

Figure 4. HO-1 facilitates lysosomal biogenesis upon oxidative stress in LECs. The primary mouse LECs were treated with 10 µM CoPP or ZnPP for 6 hours or preconditioned with 10 µM CoPP or ZnPP for 6 hours prior exposure to 100 µM H_2O_2 for 24 hours. (**A**) LAMP-1 expression levels were assessed using WB. GAPDH was used as a loading control. (**B**) LysoTracker Green DND-26 was used to visualize the lysosomes in LECs. $n = 3$, one-way ANOVA, $^*P < 0.05$, $^{***}P < 0.001$, compared with the control group; $^{\#}P < 0.05$ compared with H_2O_2-treated group. *Bar*: 50 µm.

in H_2O_2-exposed LECs. However, LC3-II/LC3-I and p62 were obviously raised when Baf-A1, an inhibitor of late-stage autophagy, was added. The pretreatment with ZnPP slightly decreased the LC3-II/LC3-I ratio and aggravated p62 accumulation, which were both elevated further after the addition of Baf-A1 (Fig. 3A). These results implied that the late-stage autophagy is interrupted in LECs challenged by H_2O_2, while HO-1 can restore the impaired autophagic flux.

Then, we measured the quantity of autophagosomes and autolysosomes with mRFP-GFP-LC3 reporter, which is regarded as a gold standard for monitoring autophagic flux and the autophagosome maturation. In comparison with the controls, the yellow and red puncta both increased in CoPP-treated cells but decreased in ZnPP-treated cells. Moreover, it is noteworthy that H_2O_2 treatment caused a dramatic elevation in yellow punctate number but a rather slight increase in the number of red punctate, suggesting the impaired autophagosome–lysosome fusion process. Interestingly, in the presence of H_2O_2, CoPP pretreatment partially restored the impaired autophagic flux, whereas ZnPP pretreatment further attenuated autophagy (Fig. 3B). All these data demonstrated that HO-1 can enhance the autophagy activity and alleviate the blockade of autophagic flux upon oxidative stress in LECs.

HO-1 Stimulates Lysosomal Biogenesis in H_2O_2-Treated LECs

To further investigate the lysosomal function, we assessed the expression levels of LAMP-1 by WB, which is widely used as a lysosomal marker. In response to CoPP, a boost in the expression level of LAMP-1 was detected, while ZnPP had the opposite effect. More important, CoPP pretreatment distinctively increased LAMP-1, which was suppressed by exposure to H_2O_2, while ZnPP pretreatment led to a further decrease of LAMP-1 (Fig. 4A). This result was also confirmed by lysotracker staining (Fig. 4B). CoPP treatment alone promoted the formation of lysosomes in LECs while ZnPP treatment slightly restrained the process. Although fewer lysosomes were observed in H_2O_2-treated groups, the preconditioning of CoPP restored the formation of lysosomes, and ZnPP pretreatment further reduced the number of lysosome. These results above suggested that HO-1 promotes lysosomal biogenesis upon oxidative damage in LECs.

HO-1 Facilitates TFEB Nuclear Translocation in LECs

TFEB is an important transcription factor that regulates autophagy. To explore whether HO-1 stimulates autophagy

Investigative Ophthalmology & Visual Science

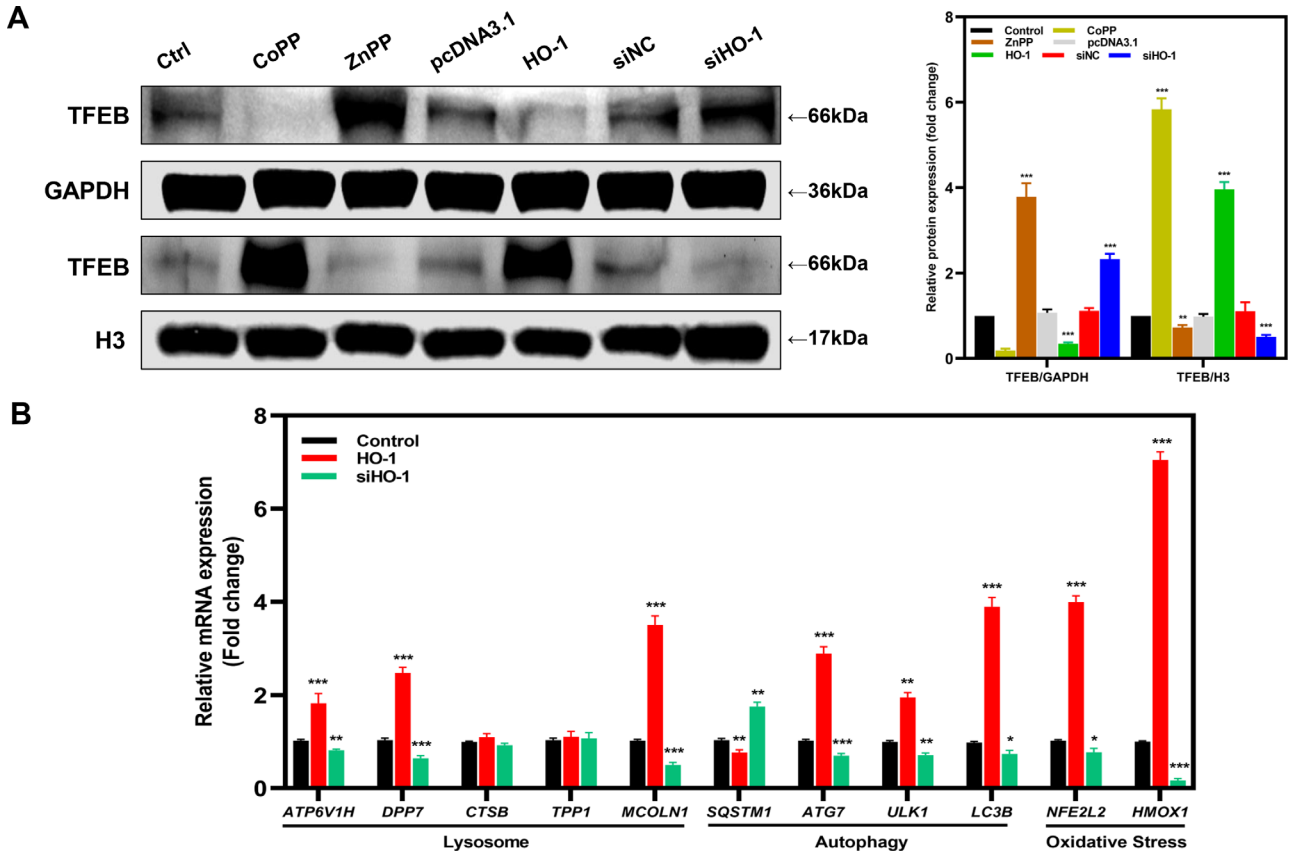

Figure 5. HO-1 promotes TFEB nuclear translocation in LECs. The primary mouse LECs were pretreated with 10 µM CoPP or ZnPP for 6 hours or transfected with pcDNA3.1-NC, pcDNA3.1-HO-1, siNC, and siHO-1, respectively. (**A**) WB displayed TFEB expression levels in cytosol and nucleus, respectively. (**B**) TFEB-targeted gene mRNA expression was detected by qPCR. pcDNA3.1-NC and siNC were used as negative control. $n = 3$, one-way ANOVA, $^{*}P < 0.05$, $^{**}P < 0.01$, $^{***}P < 0.001$, compared with the control group.

through TFEB, TFEB levels were detected through WB after treatment of 10 µM CoPP or ZnPP for 6 hours. Additionally, we also examined the expression levels of TFEB in the presence of HO-1 overexpression or knockdown. CoPP treatment and HO-1 overexpression induced the obvious downregulation of TFEB in the cytoplasm while ZnPP treatment and HO-1 knockdown upregulated the expression level of TFEB in the cytoplasm. In addition, CoPP treatment as well as HO-1 overexpression caused an obvious increase in nuclear TFEB level. On the contrary, ZnPP treatment and HO-1 knockdown led to a reduction in nuclear TFEB level (Fig. 5A).

Then, the relative mRNA expression levels of targeted genes of TFEB were measured using the qPCR assay. Compared with the controls, other than lysosomal enzyme *Tpp1*, other lysosome-related genes (*Atp6v1b*, *Dpp7*, *Ctsb*, *Mcoln1*), autophagy-related genes (*Sqstm1*, *Atg1*, *Ulk1*, *LC3b*), and oxidative stress–related genes (*Nfe2l2*, *Hmox1*) all increased significantly in response to CoPP treatment but decreased in ZnPP treatment groups ($P < 0.05$). Most notably, the gene expression of *Hmox1*, which encodes HO-1, surged almost sixfold in contrast to the control group (Fig. 5B). Collectively, these findings showed that HO-1 facilitates nuclear translocation of TFEB in LECs.

TFEB Promotes the Expression of HO-1 in LECs

To assess the effect of TFEB on HO-1 induction, we examined the expression of HO-1 in the mouse LECs under the conditions of siRNA or plasmid transfection or cotransfection by using WB and qPCR. The results showed that HO-1 expression in siTFEB-transfected groups was weakened accordingly in contrast to wild type (WT) groups, which suggested that the expression of HO-1 is mediated by TFEB (Figs. 6A–C).

It was then predicted that there existed binding sites of the transcription factor TFEB on the promoter region of *Hmox1* by the Jasper online website. Accordingly, ChIP assay demonstrated that the enrichment level of the *Hmox1* promoter pulled by TFEB antibodies markedly increased in comparison with the IgG group, which verified the binding between TFEB and *Hmox1* promoter (Fig. 6D).

HO-1 Promotes Autophagic Flux in a TFEB-Dependent Way in LECs

We further assessed how HO-1 knockdown or overexpression affects autophagy and whether autophagy induced by HO-1 is dependent on TFEB in LECs. HO-1 knockdown significantly declined the LC3-II/LC3-I ratio and increased p62 expression levels, while HO-1 overexpression had the opposite effect. However, TFEB knockdown counteracted the difference of the LC3-II/LC3-I ratio and p62 expression level among different groups. After the addition of Baf-A1, LC3-II/LC3-I ratios and p62 levels in all groups significantly increased (Fig. 7). Briefly, these data suggested that HO-1 promotes autophagic flux in a TFEB-dependent manner in LECs.

Investigative Ophthalmology & Visual Science

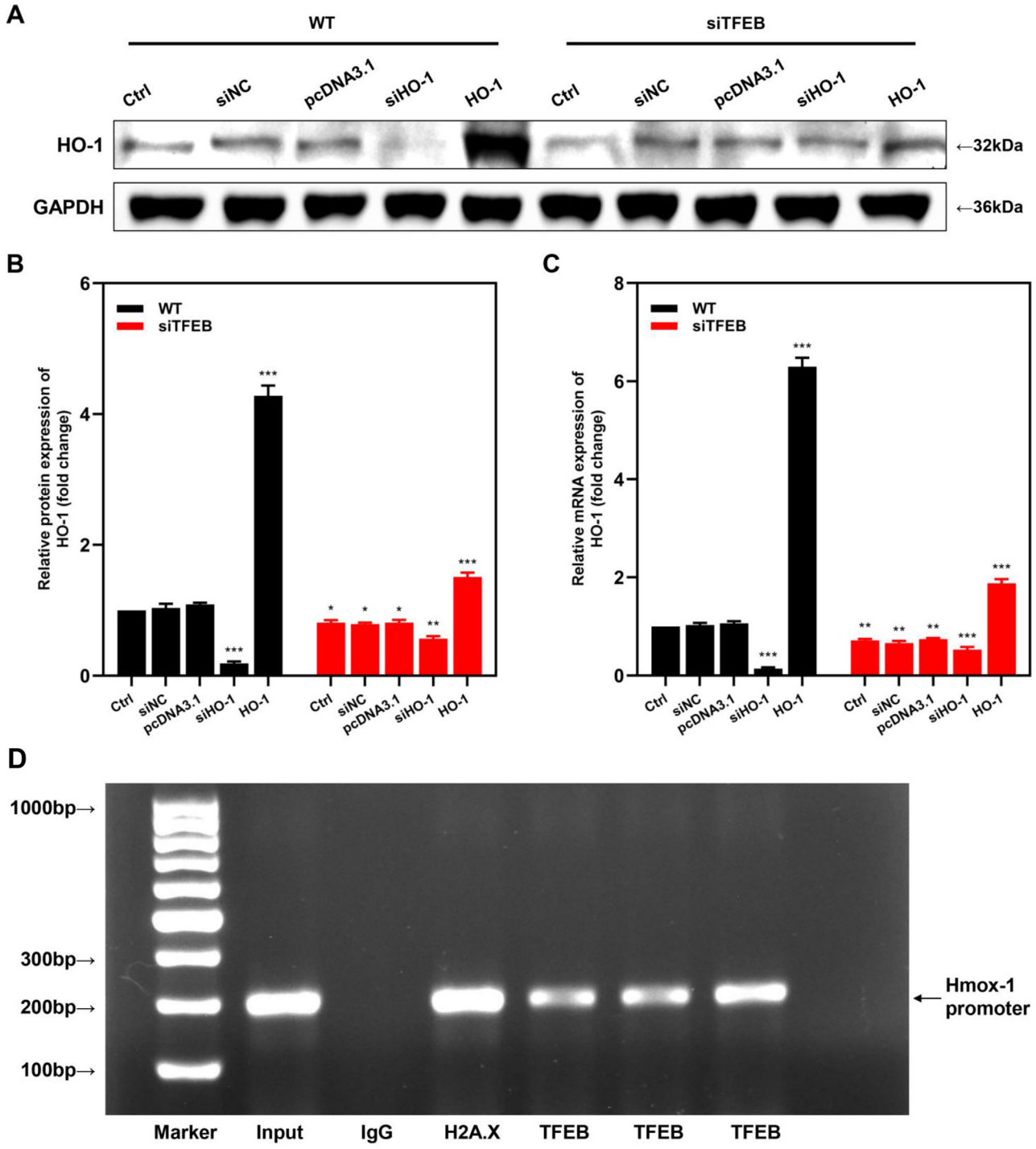

Figure 6. The expression of HO-1 is mediated by TFEB directly. Different transfection complexes were transfected into the primary mouse LECs. (**A**, **B**) Relative protein expression levels of HO-1 were assessed by WB in different groups. (**C**) Relative HO-1 mRNA expression levels were assessed by qPCR in different groups. Scrambled siRNA and empty vector (pcDNA3.1) were used as NC. (D) ChIP analysis for the binding of TFEB to the promoter region of *Hmox1* genes. IgG and H2A.X were set as the negative and positive control, respectively. $n = 3$, one-way ANOVA, $^{*}P < 0.05$, $^{**}P < 0.01$, $^{***}P < 0.001$, compared with the WT control group.

TFEB Is Required for Antioxidative and AntiAging Effects of HO-1 on LECs

To determine whether the antioxidative and antiaging effects of HO-1 were dependent on TFEB in LECs, we analyzed the intracellular ROS production and SA-β-gal activity in LECs transfected with siRNA, plasmid, or both (Fig. 8). In WT groups, siTFEB-treated groups, and H_2O_2-treated groups, HO-1 knockdown obviously increased intracellular ROS levels compared to the control group and HO-1 overexpression group. Additionally, the treatment of siTFEB transfection slightly increased ROS production in LECs, whereas

Investigative Ophthalmology & Visual Science

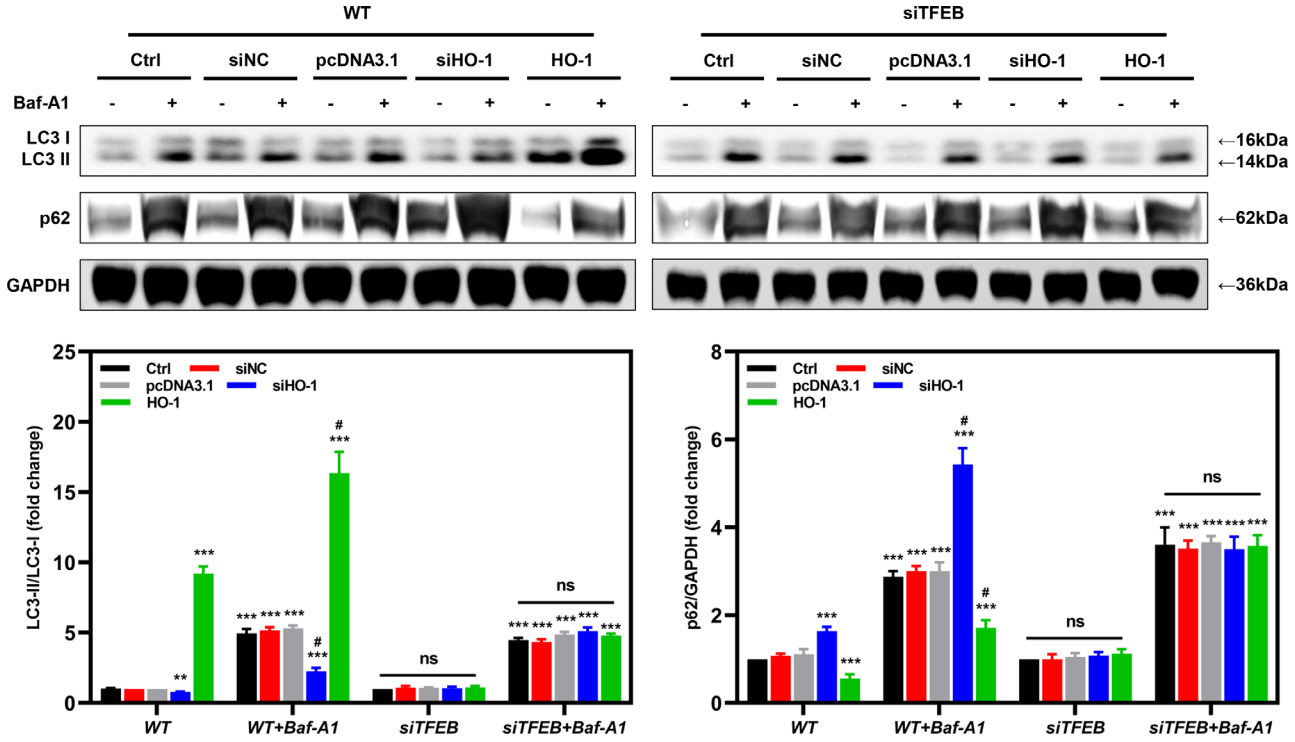

Figure 7. HO-1 promotes autophagic flux in a TFEB-dependent manner in LECs. The primary mouse LECs were transfected with different transfection complexes. WB was used to detect relative protein expression levels of LC3 and p62 in different groups. Scrambled siRNA and empty vector (pcDNA3.1) were used as NC. $n = 3$, one-way ANOVA, $^{**}P < 0.01$, $^{***}P < 0.001$, compared with the WT control group; $^{\#}P < 0.05$ compared with the WT + Baf-A1 control group.

H_2O_2 treatment caused a dramatic increase in the ROS levels. Furthermore, there was no obvious difference existing in the intracellular ROS levels with the combination treatment of H_2O_2 and siTFEB (Fig. 8A). Meanwhile, SA-β-gal assays showed that the treatment of siTFEB transfection and H_2O_2 both aggravated premature senescence of LECs. Moreover, HO-1 knockdown significantly increased the percentage of SA-β-gal–positive cells, while overexpression of HO-1 greatly decreased SA-β-gal–positive cell proportion. These results suggested that HO-1 reduces oxidative stress and delays premature senescence in a TFEB-dependent manner in LECs.

Discussion

As a result of this study, HO-1 gene expression was found to decrease in the anterior capsules of patients with ARNC, whereas the autophagy-related markers LC3 and p62 as well as senescence-related molecule p21 increased. In the mouse LEC model, we demonstrated that HO-1 restores autophagy flux impaired by H_2O_2 and prevents oxidative stress–induced senescence through facilitating nuclear translocation of TFEB (Fig. 9). Furthermore, TFEB knockdown greatly reduced the effects of HO-1 on LECs. To sum up, our study indicated that HO-1 has an essential role to play in restoring autophagic flux, alleviating oxidative stress, and delaying cell senescence in H_2O_2-exposed LECs, which are dependent on TFEB.

ARC is generally divided into three subtypes according to the morphologic characteristics under slit-lamp biomicroscopy. However, the pathogenesis of these three subtypes is different. For example, a Na^+/K^+ ATPase dysfunction and an increase in water content are widely regarded as the underlying mechanism for cortical cataract formation, while posterior subcapsular cataract is often concomitant with long-term use of corticosteroids, high myopia, and retinitis pigmentosa.[33,34] ARNC is characterized by overwhelmed oxidative stress and destroyed redox homeostasis.[35] Previously, we have demonstrated that the expression levels of several important antioxidants, including HO-1, were decreased in ARNC but not age-related cortical cataract and posterior subcapsular cataract.[26] Thus, we only selected patients with ARNC as participants in this study.

Autophagy is the main degradative pathway of damaged organelles and aggregated protein in all eukaryotic cells.[36] Ample evidence proves that autophagy and lysosomes play critical roles in protecting cells from oxidative stress and controlling intracellular quality.[36–38] However, how autophagy is involved in ARC remains obscure. In our research, LC3 and p62 were found to increase in LECs of patients with ARNC. During the autophagy process, p62 acts as a cargo receptor, which recognizes ubiquitinated cargos through the ubiquitin-associated domain and interacts with autophagosome membrane protein LC3 via the LC3-interacting region.[39] Thus, LC3 and p62 are generally used as markers for evaluating autophagy activity. After autophagosomes and lysosomes have fused, p62 is degraded along with the cargo. p62 accumulates in cells when autophagy is impaired, and its level is a hallmark of the autophagic impairment.[40,41] Therefore, combined with the increase of the autophagosome marker LC3, we suspected that autophagic impairment but not decreased autophagy activity occurs in LECs of patients with ARNC

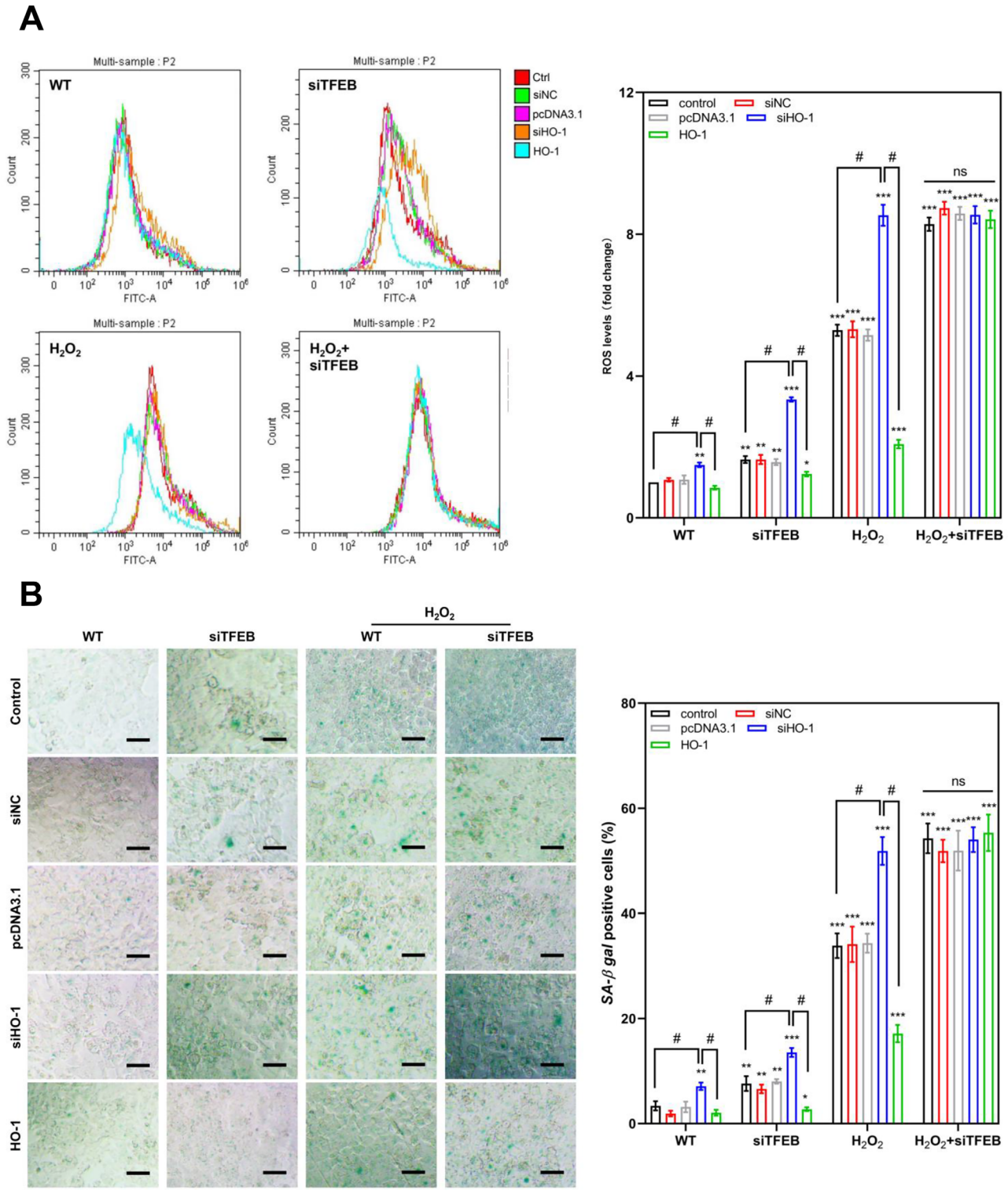

Figure 8. HO-1 reduces oxidative stress and delays premature senescence in a TFEB-dependent manner in LECs. The primary mouse LECs were transfected with different transfection complexes. (**A**) DCFH-DA staining and flow cytometry analysis were used to detect intracellular ROS levels in each group. (**B**) SA-β-gal assay was used to analyze senescent cell percentage. $n = 3$, one-way ANOVA, $^{*}P < 0.05$, $^{**}P < 0.01$, $^{***}P < 0.001$, compared with the WT control group; $^{\#}P < 0.05$. *Bar*: 50 µm.

and may contribute to the development of ARNC. Subsequently, mouse LECs were treated with H_2O_2 to construct a in vitro model of cataract, which showed senescent and autophagic features similar to human samples. Our findings agree with that of another study, in which autophagic responses of immortalized human LEC line HLE-B3, including an increase of both LC3 and p62, were induced by oxidative damage.[42] However, cataract formation can also

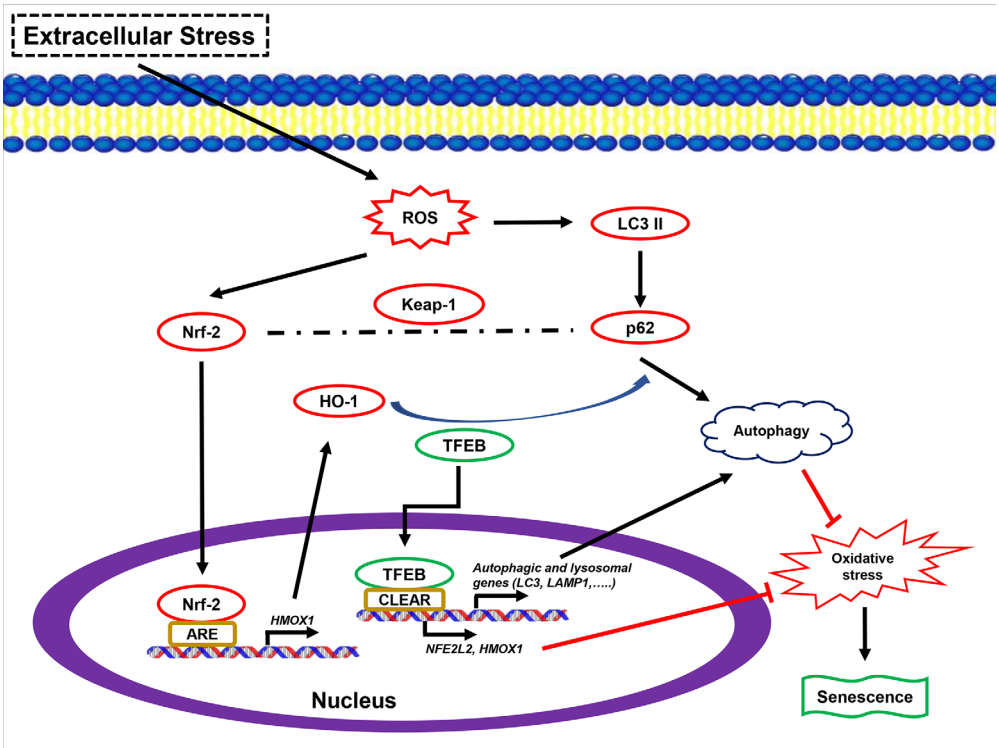

Figure 9. HO-1 effects on promoting autophagy and preventing oxidative stress against premature senescence are dependent on TFEB. The scheme reveals that extracellular stressors result in intracellular ROS accumulation, which leads to the activation of two effector molecules, namely, LC3-II and Nrf-2 (nuclear factor erythroid 2–related factor 2). LC3-II enables autophagosomes to bind autophagic substrates and proteins, which mediate cargo selectivity, including p62. As a signaling hub, p62 also interacts with Keap1 (Kelch-like ECH-associated protein 1) to mediate Nrf2 activation. The Nrf2-ARE transcriptional pathway activates the expression of *HMOX1* that encodes HO-1. HO-1 promotes autophagy and prevents oxidative stress–induced senescence through facilitating TFEB nuclear translocation, which induces gene expression associated with autophagy, lysosomes, and antioxidation.

be promoted by increased autophagy, which causes age-related cell death as well.[27] Additionally, autophagy blockage induced by high glucose has been reported in diabetic cataract,[21] but as far as we know, it has not been reported that impaired autophagic flux occurs in senile cataract.

HO-1, coded by the *HMOX1* gene, is a critical effector of stress response.[28] Many chemical and physical agents, such as heme, H_2O_2, exposure to ultraviolet-A radiation, and pro-oxidant compounds, can promote HO-1 expression.[43] However, we found that HO-1 gene expression decreased in patients with ARNC in contrast to noncataract participants. The crosstalk between HO-1 and autophagy has been investigated in other disease models. In hepatocytes, HO-1 was found to upregulate autophagy, conferring protection against hepatocyte cell death during sepsis in mice.[44] HO-1 overexpression in a mouse model of diabetes prevented cardiac failure by reestablishing normal protein kinase and improving autophagy.[45] Despite cytoprotective properties of HO-1 in the abovementioned diseases, it has been reported that activated HO-1 downregulated autophagy and apoptosis in renal cancer cells, hence diminishing therapeutic effects.[46] Therefore, an association between HO-1 and autophagy can be cell type and context specific. Many studies focused on the Nrf2/HO-1 pathway in LECs proved that the activation of Nrf2/HO-1 signaling protected LECs from oxidative stress and attenuated cataract progression.[47–49] Our previous study also demonstrated that the by-products of HO-1, biliverdin and carbon monoxide, could protect LECs from oxidative stress.[13,24–26] However, we conducted a more in-depth study on the mechanism of HO-1 function in LECs in this work, especially its downstream mechanism. Of note, we demonstrated for the first time that HO-1 can restore the autophagic flux blocked by H_2O_2 treatment and delay premature senescence in LECs.

Lysosome is the degradation center in cells and a major participant in the late stage of autophagy.[50] We found that under H_2O_2-induced oxidative stress, lysosomal function was greatly impaired. To confirm HO-1 influence on lysosomal function in LECs, transcription factors responsible for lysosomal biogenesis were investigated. TFEB is the main transcription factor involved in lysosomal biogenesis and autophagy.[19] Translocation of TFEB into the nucleus after interferon gamma immunomodulation of macrophages occurs in a HO-1–dependent fashion, as demonstrated in a previous work.[51] In line with this result, our work also demonstrated that HO-1 facilitates TFEB translocation into the nucleus to activate expression of autophagic and lysosomal genes. TFEB translocation also upregulates the expression of the *NFE2L2* gene since the TFEB binding site is present in the promoter region of the *NFE2L2* gene. Additionally, TFEB knockdown inhibits autophagy activation induced by HO-1 and reverses antioxidative and antiaging impacts of HO-1 on LECs. Recent investigations have exposed that TFEB-dependent lysosomal dysfunction impairs autophagic flux in LECs[21] and macrophages[52] in a diabetic condition, while to our knowledge, it has not been implicated in senescence-associated diseases. Damaged organelles, such as mitochondria, may

not be degraded properly due to TFEB-mediated lysosomal dysfunction, which ultimately increases ROS generation.[53] Then the ROS/p53/p21 pathway, which promotes cellular senescence, would be triggered by an increase in ROS levels.[54] In the present study, HO-1 was proved to downregulate p53 and p21 expression and decrease the senescent LEC percentage under H_2O_2-induced oxidative stress. Therefore, excessive oxidative stress can cause lysosomal defects and impaired autophagic flux, which might lead to further generating ROS and promoting cellular senescence, while HO-1 can facilitate autophagy and prevent oxidative stress–induced senescence in a TFEB-dependent way.

In conclusion, our study reveals that HO-1 restores autophagic flux and delays cellular senescence under excessive oxidative stress, which is dependent on TFEB. Additionally, TFEB could promote the transcription and expression of HO-1 directly via binding to the *Hmox1* promoter in LECs. These results propose that a combination of antioxidants and lysosomal restoration may be an effective strategy for ARC prevention. Our research offers a fresh perspective on the pathogenesis and treatment of senile cataract.

Acknowledgments

Supported by Shanghai's Innovation for Science and Technology (20Y11910900).

All data utilized and/or analyzed in this work can be obtained from the corresponding author.

Institutional review board and ethical Committee of Shanghai East Board, as well as the China Ethics Committee for Registration Clinical Trials, all gave their approval to use human samples in this investigation (ChiCTR2000036059). Participants gave their written consent before any clinical procedures were performed, as required by the Declaration of Helsinki. Tongji University's animal care ethics committee gave its approval to the experimental methodologies and animal care procedures. In addition, all procedures complied with the ARVO animal statement.

Disclosure: **L. Wang**, None; **W. Lou**, None; **Y. Zhang**, None; **Z. Chen**, None; **Y. Huang**, None; **H. Jin**, None

References

1. Cicinelli MV, Buchan JC, Nicholson M, Varadaraj V, Khanna RC. Cataracts. *Lancet*. 2022;401(10374):377–389.
2. Asbell PA, Dualan I, Mindel J, Brocks D, Ahmad M, Epstein S. Age-related cataract. *Lancet*. 2005;365(9459):599–609.
3. Lee CM, Afshari NA. The global state of cataract blindness. *Curr Opin Ophthalmol*. 2017;28(1):98–103.
4. Yan Y, Yu H, Sun L, et al. Laminin $\alpha 4$ overexpression in the anterior lens capsule may contribute to the senescence of human lens epithelial cells in age-related cataract. *Aging (Albany NY)*. 2019;11(9):2699–2723.
5. Chen M, Fu Y, Wang X, et al. Metformin protects lens epithelial cells against senescence in a naturally aged mouse model. *Cell Death Discov*. 2022;8(1):8.
6. Cai M, Li J, Lin S, et al. Mitochondria-targeted antioxidant peptide SS31 protects cultured human lens epithelial cells against oxidative stress. *Curr Eye Res*. 2015;40(8):822–829.
7. Roy AL, Sierra F, Howcroft K, et al. A blueprint for characterizing senescence. *Cell*. 2020;183(5):1143–1146.
8. Gorgoulis V, Adams PD, Alimonti A, et al. Cellular senescence: defining a path forward. *Cell*. 2019;179(4):813–827.
9. Spector A. Oxidative stress-induced cataract: mechanism of action. *FASEB J*. 1995;9(12):1173–1182.
10. Lim JC, Caballero Arredondo M, Braakhuis AJ, Donaldson PJ. Vitamin C and the lens: new insights into delaying the onset of cataract. *Nutrients*. 2020;12(10):3142.
11. Spector A, Garner WH. Hydrogen peroxide and human cataract. *Exp Eye Res*. 1981;33(6):673–681.
12. Chen M, Zhang C, Zhou N, Wang X, Su D, Qi Y. Metformin alleviates oxidative stress-induced senescence of human lens epithelial cells via AMPK activation and autophagic flux restoration. *J Cell Mol Med*. 2021;25(17):8376–8389.
13. Huang Y, Liu Y, Yu S, et al. Biliverdin reductase A protects lens epithelial cells against oxidative damage and cellular senescence in age-related cataract. *Oxid Med Cell Longev*. 2022;2022:5628946.
14. Rubinsztein DC, Marino G, Kroemer G. Autophagy and aging. *Cell*. 2011;146(5):682–695.
15. Kitada M, Koya D. Autophagy in metabolic disease and ageing. *Nat Rev Endocrinol*. 2021;17(11):647–661.
16. Shirakabe A, Ikeda Y, Sciarretta S, Zablocki DK, Sadoshima J. Aging and autophagy in the heart. *Circ Res*. 2016;118(10):1563–1576.
17. Wignes JA, Goldman JW, Weihl CC, Bartley MG, Andley UP. p62 expression and autophagy in αB-crystallin R120G mutant knock-in mouse model of hereditary cataract. *Exp Eye Res*. 2013;115:263–273.
18. Makley LN, McMenimen KA, DeVree BT, et al. Pharmacological chaperone for α-crystallin partially restores transparency in cataract models. *Science (New York, NY)*. 2015;350(6261):674–677.
19. Settembre C, Di Malta C, Polito VA, et al. TFEB links autophagy to lysosomal biogenesis. *Science (New York, NY)*. 2011;332(6036):1429–1433.
20. Li J, Sun Q, Qiu X, et al. Downregulation of AMPK dependent FOXO3 and TFEB involves in the inhibition of autophagy in diabetic cataract. *Curr Eye Res*. 2022;47(4):555–564.
21. Sun Y, Wang X, Chen B, et al. TFEB-mediated lysosomal restoration alleviates high glucose-induced cataracts via attenuating oxidative stress. *Invest Ophthalmol Vis Sci*. 2022;63(6):26.
22. Abraham NG, Kappas A. Pharmacological and clinical aspects of heme oxygenase. *Pharmacol Rev*. 2008;60(1):79–127.
23. Ryter SW, Alam J, Choi AM. Heme oxygenase-1/carbon monoxide: from basic science to therapeutic applications. *Physiol Rev*. 2006;86(2):583–650.
24. Huang Y, Ma T, Ye Z, et al. Carbon monoxide (CO) inhibits hydrogen peroxide (H2O2)-induced oxidative stress and the activation of NF-kappaB signaling in lens epithelial cells. *Exp Eye Res*. 2018;166:29–39.
25. Huang Y, Ye Z, Ma T, et al. Carbon monoxide (CO) modulates hydrogen peroxide (H2O2)-mediated cellular dysfunction by targeting mitochondria in rabbit lens epithelial cells. *Exp Eye Res*. 2018;169:68–78.
26. Huang Y, Li J, Li W, Ai N, Jin H. Biliverdin/bilirubin redox pair protects lens epithelial cells against oxidative stress in age-related cataract by regulating NF-kappaB/iNOS and Nrf2/HO-1 pathways. *Oxid Med Cell Longev*. 2022;2022:7299182.
27. Zheng Y, Yang X, Wu S, et al. Paired box gene 6 regulates heme oxygenase-1 expression and mitigates hydrogen peroxide-induced oxidative stress in lens epithelial cells. *Curr Eye Res*. 2022;47(11):1516–1524.
28. Ryter SW. Heme oxgenase-1, a cardinal modulator of regulated cell death and inflammation. *Cells*. 2021;10(3):515.
29. Shan Y, Pepe J, Lu TH, Elbirt KK, Lambrecht RW, Bonkovsky HL. Induction of the heme oxygenase-1 gene by metalloporphyrins. *Arch Biochem Biophys*. 2000;380(2):219–227.

30. Huang Y, Ye Z, Yin Y, et al. Cataract formation in transgenic HO-1 G143H mutant mice: involvement of oxidative stress and endoplasmic reticulum stress. *Biochem Biophys Res Commun*. 2021;537:43–49.
31. Tchakarska G, Sola B. The double dealing of cyclin D1. *Cell Cycle (Georgetown, Tex)*. 2020;19(2):163–178.
32. Barnes PJ, Baker J, Donnelly LE. Cellular senescence as a mechanism and target in chronic lung diseases. *Am J Respir Crit Care Med*. 2019;200(5):556–564.
33. Richardson RB, Ainsbury EA, Prescott CR, Lovicu FJ. Etiology of posterior subcapsular cataracts based on a review of risk factors including aging, diabetes, and ionizing radiation. *Int J Radiat Biol*. 2020;96(11):1339–1361.
34. Pau H. Cortical and subcapsular cataracts: significance of physical forces. *Ophthalmologica*. 2006;220(1):1–5.
35. Truscott RJW. Age-related nuclear cataract-oxidation is the key. *Exp Eye Res*. 2005;80(5):709–725.
36. Mizushima N, Komatsu M. Autophagy: renovation of cells and tissues. *Cell*. 2011;147(4):728–741.
37. Morishita H, Eguchi S, Kimura H, et al. Deletion of autophagy-related 5 (Atg5) and Pik3c3 genes in the lens causes cataract independent of programmed organelle degradation. *J Biol Chem*. 2013;288(16):11436–11447.
38. Mizushima N, Yoshimori T, Ohsumi Y. The role of Atg proteins in autophagosome formation. *Annu Rev Cell Dev Biol*. 2011;27:107–132.
39. Hennig P, Fenini G, Di Filippo M, Karakaya T, Beer HD. The pathways underlying the multiple roles of p62 in inflammation and cancer. *Biomedicines*. 2021;9(7):707.
40. Sánchez-Martín P, Komatsu M. p62/SQSTM1—steering the cell through health and disease. *J Cell Sci*. 2018;131(21):jcs222836.
41. Jiang P, Mizushima N. LC3- and p62-based biochemical methods for the analysis of autophagy progression in mammalian cells. *Methods*. 2015;75:13–18.
42. Zhou J, Yao K, Zhang Y, et al. Thioredoxin binding protein-2 regulates autophagy of human lens epithelial cells under oxidative stress via inhibition of Akt phosphorylation. *Oxid Med Cell Longev*. 2016;2016:4856431.
43. Ryter SW, Choi AMK. Targeting heme oxygenase-1 and carbon monoxide for therapeutic modulation of inflammation. *Transl Res*. 2016;167(1):7–34.
44. Carchman EH, Rao J, Loughran PA, Rosengart MR, Zuckerbraun BS. Heme oxygenase-1-mediated autophagy protects against hepatocyte cell death and hepatic injury from infection/sepsis in mice. *Hepatology*. 2011;53(6):2053–2062.
45. Zhao Y, Zhang L, Qiao Y, et al. Heme oxygenase-1 prevents cardiac dysfunction in streptozotocin-diabetic mice by reducing inflammation, oxidative stress, apoptosis and enhancing autophagy. *PLoS One*. 2013;8(9):e75927.
46. Banerjee P, Basu A, Wegiel B, et al. Heme oxygenase-1 promotes survival of renal cancer cells through modulation of apoptosis- and autophagy-regulating molecules. *J Biol Chem*. 2012;287(38):32113–32123.
47. Yang T, Lin X, Li H, et al. Acetyl-11-keto-beta boswellic acid (AKBA) protects lens epithelial cells against H2O2-induced oxidative injury and attenuates cataract progression by activating Keap1/Nrf2/HO-1 signaling. *Front Pharmacol*. 2022;13:927871.
48. Chowdhury A, Balogh E, Ababneh H, Tóth A, Jeney V. Activation of Nrf2/HO-1 antioxidant pathway by heme attenuates calcification of human lens epithelial cells. *Pharmaceuticals (Basel)*. 2022;15(5):493.
49. Ma T, Chen T, Li P, et al. Heme oxygenase-1 (HO-1) protects human lens epithelial cells (SRA01/04) against hydrogen peroxide (H2O2)-induced oxidative stress and apoptosis. *Exp Eye Res*. 2016;146:318–329.
50. Xu H, Ren D. Lysosomal physiology. *Annu Rev Physiol*. 2015;77:57–80.
51. Singh N, Kansal P, Ahmad Z, et al. Antimycobacterial effect of IFNG (interferon gamma)-induced autophagy depends on HMOX1 (heme oxygenase 1)-mediated increase in intracellular calcium levels and modulation of PPP3/calcineurin-TFEB (transcription factor EB) axis. *Autophagy*. 2018;14(6):972–991.
52. Yuan Y, Chen Y, Peng T, et al. Mitochondrial ROS-induced lysosomal dysfunction impairs autophagic flux and contributes to M1 macrophage polarization in a diabetic condition. *Clin Sci (Lond)*. 2019;133(15):1759–1777.
53. Zhang Z, Yan J, Bowman AB, Bryan MR, Singh R, Aschner M. Dysregulation of TFEB contributes to manganese-induced autophagic failure and mitochondrial dysfunction in astrocytes. *Autophagy*. 2020;16(8):1506–1523.
54. Zhang Y, Peng X, Xue M, et al. SARS-COV-2 spike protein promotes RPE cell senescence via the ROS/P53/P21 pathway. *Biogerontology*. 2023;24(5):813–827.

Investigative Ophthalmology & Visual Science